Growth and characterization of aligned carbon nanotubes from patterned nickel nanodots and uniform thin films

J.G. Wen, Z.P. Huang, D.Z. Wang, J.H. Chen, S.X. Yang, and Z.F. Ren[a)]
Department of Physics, Boston College, Chestnut Hill, Massachusetts 02467

J.H. Wang
Department of Chemistry, State University of New York, Buffalo, New York 14260

L.E. Calvet, J. Chen, J.F. Klemic, and M.A. Reed
Departments of Applied Physics, Electrical Engineering and Physics, Yale University, New Haven, Connecticut 06520-8284

(Received 6 March 2001; accepted 4 September 2001)

Microstructures of well-aligned multiwall carbon nanotubes grown on patterned nickel nanodots and uniform thin films by plasma-enhanced chemical vapor deposition have been studied by electron microscopy. It was found that growth of carbon nanotubes on patterned nickel nanodots and uniform thin films is different. During growth of carbon nanotubes, a nickel particle sits at the tip of each nanotube, and its [220] is preferentially oriented along the plasma direction, which can be explained by a channeling effect of ions coming into nickel particles in plasma. The alignment of nanotubes is induced by the electrical field direction relative to substrate surface.

I. INTRODUCTION

Individual single-wall carbon nanotubes (SWNTs) and multiwall carbon nanotubes (MWNTs) have been demonstrated to be excellent electron emitters due to their large aspect ratio, high chemical stability, and small end radius.[1–5] However, there has been no successful alignment of single-wall individual or bundle nanotubes. Fortunately, the growth of large arrays of well-aligned MWNTs in an area up to inches in dimension has been achieved on glass,[6] nickel,[7] and silicon[8] by plasma-enhanced chemical vapor deposition (PECVD), and on silica,[9] porous silicon,[10] and porous alumina[11,12] by chemical vapor deposition. However, the emission property of these arrays is not satisfactory, which is probably due to the high site density ($>10^9/cm^2$) leading to small electrical enhancement at the tips. A site density of about $10^7/cm^2$ has been calculated to be the right number for optimal electron emission properties in the sense of both emission site and current density.[13] The growth of arrays of well-aligned freestanding MWNTs with sharp tips and controlled diameter, length, and site spacing has been achieved through PECVD. This method provides a new approach for obtaining optimal emitter density of carbon nanotubes.

For the aligned MWNTs grown on a uniform Ni layer, a catalyst particle at the tip of each nanotube was observed.[6–8] Furthermore, the particle had a preferential orientation relative to the catalytically active surface,[14] which was explained by a model that Ni surfaces except (220) will be quickly covered up and the only exposed surface is the catalytically active (220) surface. The authors also attributed the alignment of the subsequent carbon nanotubes to the catalytically active surface mechanism. If the catalytically active surface mechanism is correct, then orientation of aligned nanotubes should not be affected by plasma direction. However, recent observation of a titled growth of aligned MWNTs arrays by changing direction of direct current (dc) plasma,[8] further confirmed by microwave plasma,[15] suggested that the catalytically active surface mechanism is not completely correct. In this paper, we report the studies on the growth and microstructural characterization of aligned MWNTs from patterned nickel nanodots and uniform thin films grown by PECVD. The preferential orientation of Ni particles was found because of the channeling effect, and the alignment of MWNTs was found due to the electrical field direction relative to the substrate surface.

II. EXPERIMENTAL

Synthesis of such aligned MWNTs from patterned nickel nanodots and uniform thin films begins first with patterning of thin film nickel (Ni) on a *p*-type boron-doped 9.5 Ω-cm (100) silicon substrate.[8,16] Then a bilayer e-beam resist was patterned by electron beam lithography to open a small window for nickel nanodot

a)Address all correspondence to this author.
e-mail: renzh@bc.edu

deposition. A thin Ni layer of 15 nm was deposited by electron beam evaporation. The final Ni pattern remained after resist/film liftoff in acetone. Finally, the patterned substrate was loaded into a PECVD system with a base pressure below 10^{-6} torr. Growth was performed at a pressure of 1–10 torr with a mixture gas of acetylene: ammonia of 40:160. The growth time was about 5 min, and the sample temperature was estimated below 600 °C because no obvious deformation occurred when commercial glasses with strain points of 500 to 590 °C were used as substrates.

Cross-sectional transmission electron microscopy (TEM) sample preparation was as follows: The as-grown film with aligned single freestanding nanotubes was penetrated with a mixture of M-Bond 610 epoxy resin (South Bay Technology, CA) and acetone to provide mechanical stiffness. The sample was first mechanically ground close to an array of the carbon nanotubes by a tripod (a precise grinding tool), then thinned from another side to about 10 μm thick. During the ion milling process, the ion beam emitted from only the substrate side such that the tip structure was prevented from direct ion milling. To investigate cross-sectional microstructures of an array of single freestanding MWNTs with a diameter of about 200 nm and spacing of about 2 μm, one has to finish ion milling exactly on the array of MWNTs. A cross-sectional TEM sample preparation method, which enabled us to be able to obtain large area and precise control of the final ion polishing by color fringes, was employed.[17] Before the sample was ion milled to electron transparency, frequent checking under TEM was conducted to finally reach the array of single freestanding carbon nanotubes. TEM and scanning electron microscopic (SEM) studies were carried out on a JEOL 4000 EX (Tokyo, Japan) transmission electron microscope operating at 400 keV and a JEOL 6340 FEG scanning electron microscope, respectively.

III. RESULTS AND DISCUSSION

Our early report shows that synthesis of large arrays of well-aligned MWNTs was achieved by PECVD on a large-area uniform catalytic Ni layer.[6–8] To investigate the hollow nature of the aligned MWNTs, a film of aligned MWNTs grown on a large area Ni layer was filled by M-Bond epoxy resin and then ion milled at a graze angle with respect to the film surface till MWNTs were exposed. Figure 1 shows a SEM top-view image of such an ion-milled sample. Three types of image contrast were observed in Fig. 1: (i) full bright circle marked by A, indicating that the nanotube was not exposed yet; (ii) bright circle with a dark spot at the center marked by B, indicating that the Ni particle at the tip was completely milled away; and (iii) gray circle with a bright spot at the center marked by C, indicating that the upper part of the Ni particle was milled away with the lower part still remaining at the tip. The distances between MWNTs are 200 nm on average. They correspond to a site density of $5 \times 10^8/\text{cm}^2$, which is too high compared to the optimal site density for field emission.

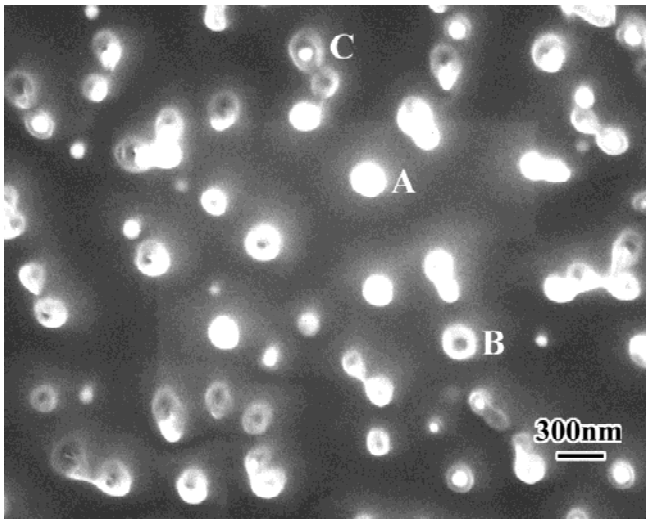

FIG. 1. Top-view SEM image of well-aligned MWNTs grown on a large area Ni layer. The film was filled by epoxy resin and then ion milled at a graze angle with respect to the film surface. The average site density is around $5 \times 10^8/\text{cm}^2$. Three types of image contrast marked by A, B, and C are explained in the text.

It is known that carbon nanotubes grow only with Ni, Fe, or Co catalysts. This implies that growth of an array of single freestanding MWNTs becomes possible if a large-area Ni layer is patterned into nanodots.[16] Figure 2 shows SEM side-view images of the aligned MWNTs from patterned nickel nanodots and uniform thin film. Figure 2(a) is a low-magnification SEM image showing an arrangement of different patterning dimensions of polycrystalline Ni on a Si substrate. Ni film is imaged as white contrast in this image. Figures 2(b), 2(c), and 2(d) show high-magnification images of aligned MWNTs grown on areas corresponding to the right large white area, one of the patterns in the top two line patterns, one of the patterns in the bottom line patterns, respectively, in Fig. 2(a). The structure of single freestanding MWNT as seen in Fig. 2(d) accurately reflects the spacing of the lithographically patterned Ni dots. This enables us to be able to control the site density of single freestanding MWNTs. A variation in the height is observed while the base diameters are approximately uniform. The variation in height is probably due to a nonuniformity of the activity of nickel nanodots, which can be improved by thorough cleaning after the resist liftoff. The base diameter can be tuned by changing the dimension of patterned Ni dots as discussed later.

The Ni dots' diameter is around 200 nm as shown in Fig. 2(d) while the dimension of other patterns of Ni layer is over 10 μm. All carbon nanotubes are well

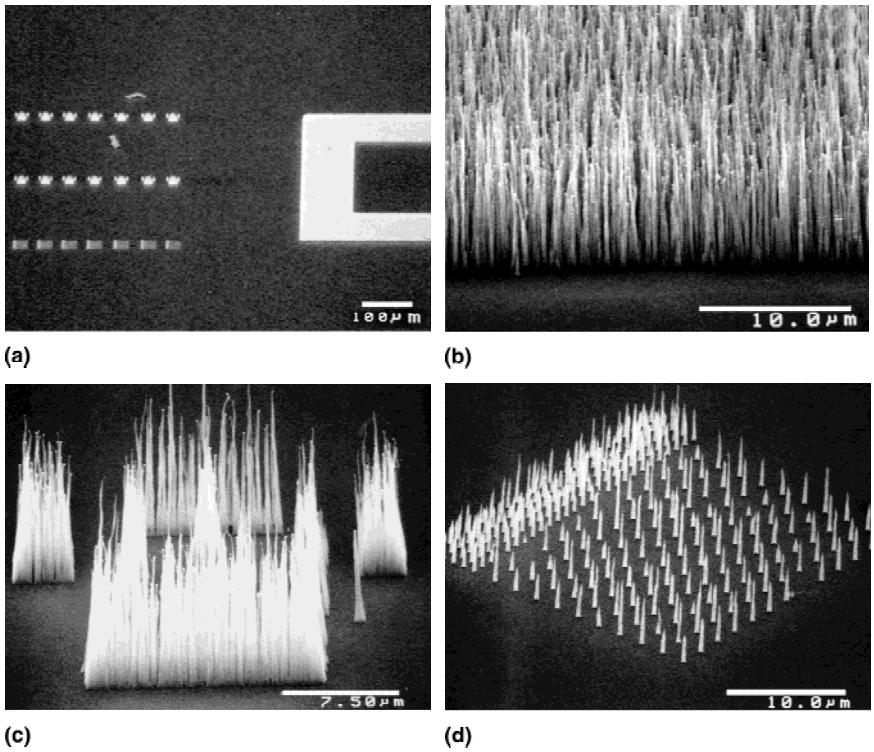

FIG. 2. (a) Low-magnification SEM image showing an arrangement of different patterning dimensions of polycrystalline Ni on a Si substrate. (b,c,d) High-magnification images of aligned standing carbon nanotubes grown on areas corresponding to the right, the left up, and the left bottom parts in (a). Ni particles can be observed on nanotubes grown on a large area Ni layer shown in (b) and (c). Tips of single freestanding nanotube on nickel nanodots are sharp and tapered, and Ni particles were not observed by SEM as shown in (d).

aligned and perpendicular to substrate surfaces in this case. From this figure, we found that growth of carbon nanotubes on nickel nanodots was different from that on a large area Ni, depending on the pattern dimension of a Ni layer. Nanotubes grown on a large-area Ni layer shown in Fig. 2(b) are longer with uniform diameter from the bottom to the tip. Ni particles can be found at tips of these nanotubes. However, nanotubes grown on nickel nanodots shown in Fig. 2(d) are shorter and their tips are sharp. No Ni particles can be observed on these tips in the SEM image.

An array of single freestanding MWNTs are characterized by cross-sectional TEM to understand microstructures of the tip, the middle part, and the interface between substrate and nanotube. Figure 3 shows a cross-sectional TEM image of an array of single freestanding MWNTs in a low magnification. The length of MWNTs are in the range of 8 to 10 μm. All single freestanding MWNTs taper at the tip as shown in Fig. 4(a). This is distinct from the early observation of a flat tip grown on large-area uniform Ni layer.[6–8] Fig. 4(b) shows a high-resolution transmission electron microscopic (HRTEM) image of a single freestanding MWNT tip. The number of walls is less than 10 at the tip. The radius of the curvature at the tip is about 2 nm. All tips of freestanding MWNTs imaged are capped by a graphitic dome. At each

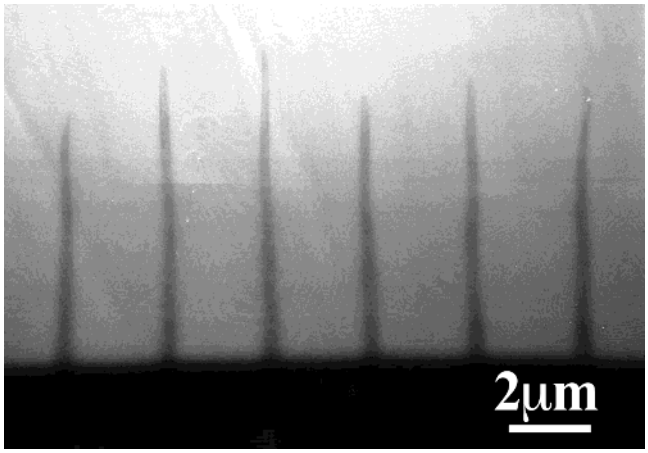

FIG. 3. Cross-sectional TEM image of an array of single freestanding MWNTs in low-magnification.

tip of single freestanding MWNT, one can always find an encapsulated single-crystalline Ni cylinder with a diameter of about 10 nm. Composition analysis by energy-dispersive x-ray spectroscopy with a small probe shows that the particle is Ni. Nanodiffraction on the Ni particle shows that its orientation along the nanotube axis is [220]. One of {222} lattice fringes can be seen in the HRTEM image shown in Fig. 4(b).

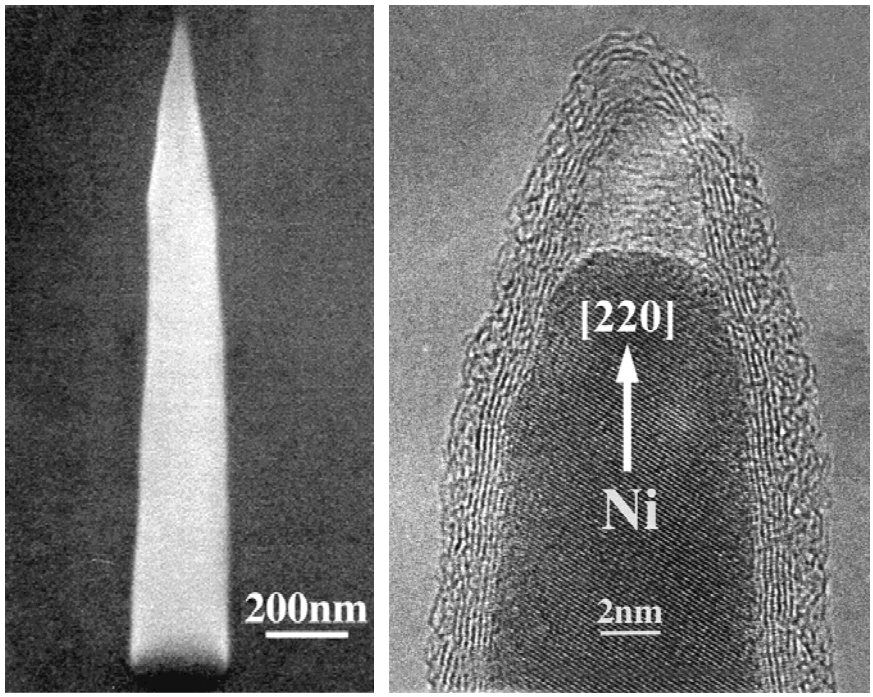

FIG. 4. (a) Large-magnification image of the single freestanding nanotube shown in Fig. 2(d). A sharp tip can be observed. (b) Cross-sectional HRTEM image of a single freestanding nanotube tip. A single-crystalline Ni cylinder with its [220] axis oriented along the nanotube axis (diameter of about 10 nm) is encapsulated. Diameters of graphitic dome and Ni tip are about 3 and 8 nm, respectively. Lattice fringes in the center of (b) correspond to (222) planes of the Ni particle.

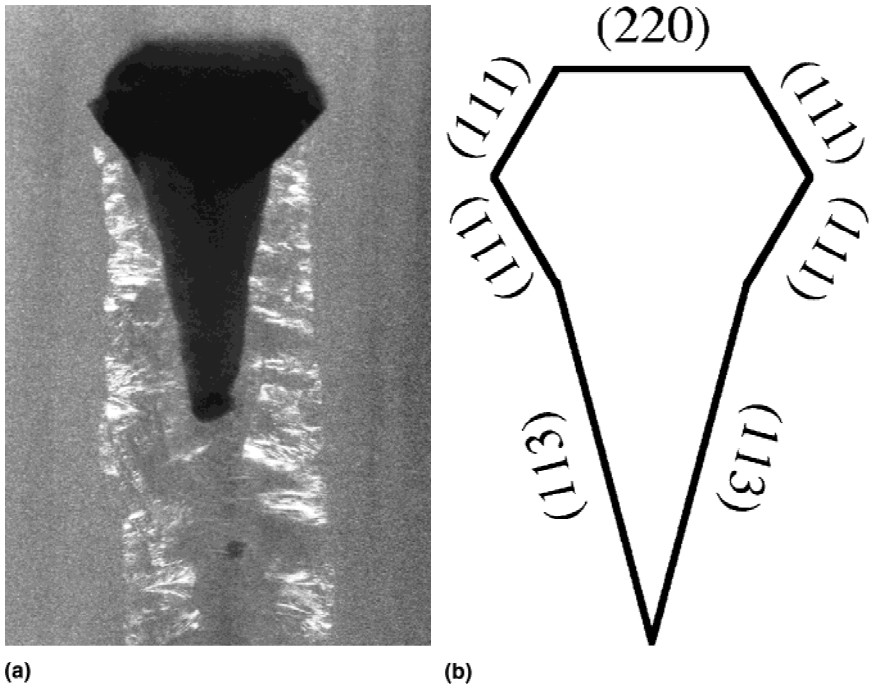

FIG. 5. (a) Typical low-magnification dark-field (002 reflection of the nanotube) image of a MWNT tip grown on large area Ni layer. The Ni particle shows a drill shape with a relatively flat top of a (220) plane. (b) Several facets of the Ni particle are indexed.

Microstructures of Ni particles and MWNTs grown on a large-area Ni layer were also investigated by cross-sectional TEM. Figure 5(a) shows a dark-field TEM image of the tip structure of a MWNT grown on a large area Ni layer using diffraction (002) of the MWNT. Most of the Ni particles situated on the top of MWNTs on a large area Ni layer show a drill shape with a relatively flat top. This is consistent with SEM images shown in Figs. 2(b) and 2(c) and the results observed by Kuang *et al.*[14] Nanodiffraction of these Ni particles shows that the flat top surface is (220). Several facets of the Ni particle on the right MWNT are indexed as shown in Fig. 5(b). Therefore, Ni particles are preferentially [220] orientated along the tube axis. No graphitic layer was observed on (220)

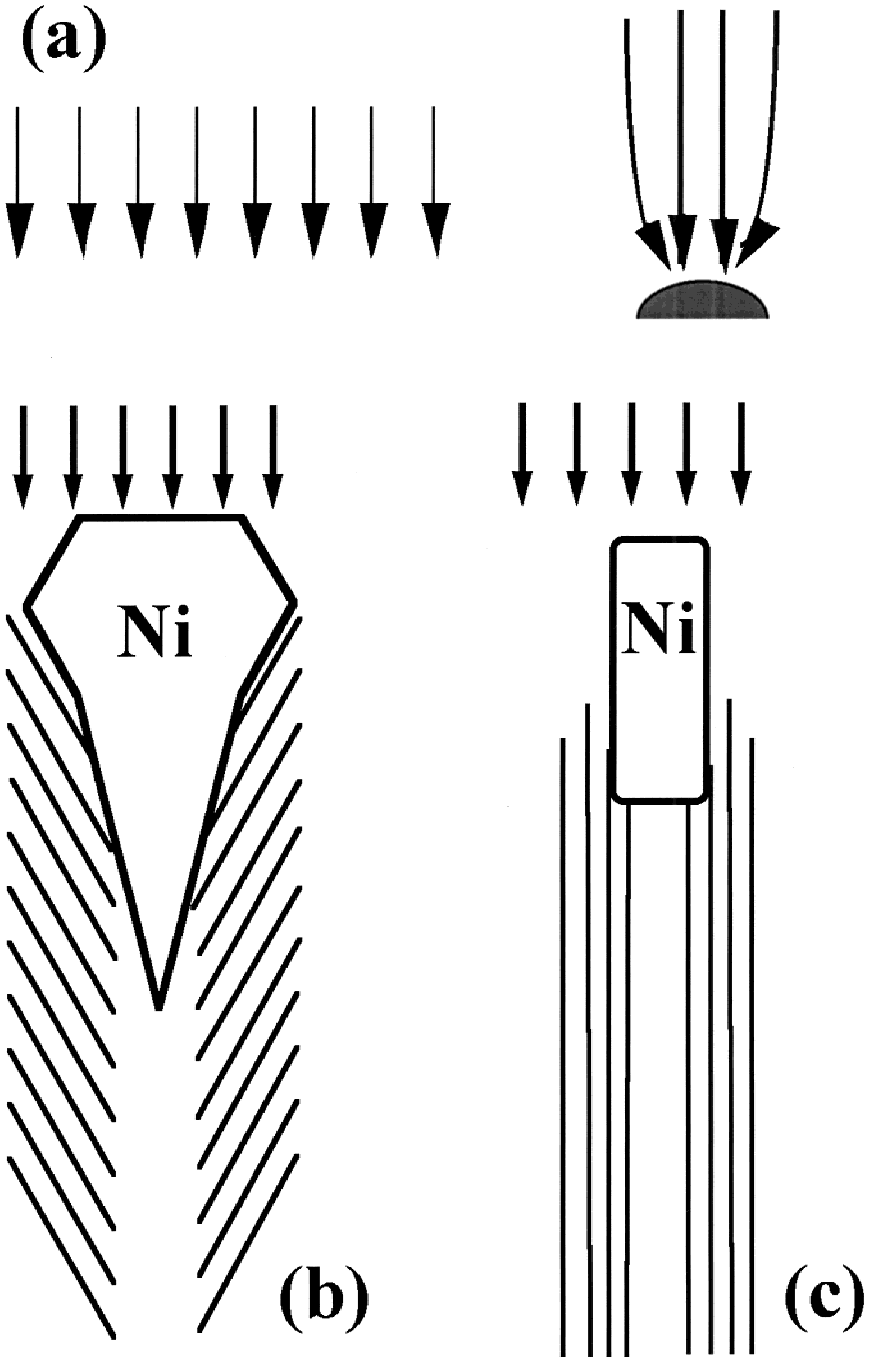

FIG. 6. (a) Schematic diagram of a focus effect of the coming bombardment ions at nickel nanodots. The local temperature at nickel nanodots is slightly higher than that on a large-area Ni layer. (b,c) Schematic diagrams of different growth modes of MWNTs with large faceted Ni particles and small Ni particles, respectively.

faceted surface, indicating the (220) surface is catalytically active and the diffusion rate of carbon atoms on it is high, as pointed by Kuang *et al.*[14]

Different growth of MWNTs on a large-area Ni layer and nickel nanodots may result from the plasma heating effect. The voltage applied on dc plasma is concentrated in a thin layer near the surface of sample since the plasma is electrically conductive. The distribution of voltage drop on a large-area Ni layer and nickel nanodots is different. It can focus the coming bombardment ions at nickel nanodots and then enhance the local temperature at nickel nanodots.[18] This is schematically shown in Fig. 6(a). It is often observed that two walls imaged on both side of MWNTs grown on a large-area Ni layer are not parallel with each other, with a tilt angle of less than a few degrees. Therefore, "bamboo" structures are often observed. But single freestanding MWNTs are free from such defects. The difference may be due to the different catalyst size and local temperature. Faceted Ni particles may easily result in a cone-type graphitic structure as schematically shown in Fig. 6(b). When the growth temperature is high, a nanotube grows as a prefect structure as shown in Fig. 6(c). There are no graphitic layers on the Ni particles at tips of MWNTs grown on a large-area Ni layer while single freestanding nanotubes are capped. This could be explained by the fact that the Ni particles at tips of MWNTs grown on a large-area Ni layer are (220) faceted as discussed above. One more possible reason is that Ni particles at nanotube tips on a large-area Ni layer are so large that Ni particles can not be capped.

The reason why most of Ni particles are [220] oriented along the applied dc plasma direction could be explained by a channeling effect in the plasma. In the Ni crystal with a face-centered cubic structure, Ni atoms are close-packed along the [220] axis, so [220] is the channeling direction of the Ni crystal. During the growth, Ni particles preferentially orient their channeling direction [220] along the direction of coming ions in the dc plasma to minimize the interaction energy between bombardment ions and Ni particles.[19] This is the same principle as that used in ion-beam-assisted deposition to biaxially align buffer layers for $YBa_2Cu_3O_7$ films on nonepitaxial substrates.[20]

From the results described above, one can see that MWNTs are perpendicular to the substrate surface plane and Ni articles are preferentially [220] orientated along the tube axis. To understand the alignment mechanism for both MWNTs and orientation of Ni particles, the substrate was tilted away from the applied dc plasma. It was found that MWNTs grow along the applied dc plasma direction as reported previously.[8] Ni particles at the tips of these MWNTs also orient the [220] axis along the applied dc plasma direction. This further confirms the orientation mechanism of Ni particles by plasma. Figure 7 shows a SEM image of MWNTs grown on a tungsten filament coated by a thin Ni layer. Most MWNTs are aligned along the dc plasma direction even at two sides of the wire. It is different from the reported result that MWNTs synthesized under microwave plasma grow perpendicular to the local surface.[15] The difference may result from different bias voltage of dc plasma and self-bias voltage of microwave plasma. Local electrical field is always perpendicular to local surface at substrate, especially in the case of low bias voltage (around 10 V) such as in microwave PECVD. High bias voltage (around 300 V) in the dc plasma case results in electrical field roughly parallel to the macroscopic electrical field, the applied dc plasma direction, as soon as it is slightly away from substrate surfaces. During the growth, carbon nanotubes are forced to align along local electrical field direction by the electrostatic force caused by bias voltage.[15,21] Moreover, Ni particles at the tips of nanotubes behave as an "umbrella" to protect MWNTs from the bombardment of coming ions, in the case of large bias voltage and a tip growth mode.

Microstructures at the interface between the bottom of freestanding MWNT and silicon substrate were also investigated by cross-sectional TEM. Figure 8(a) shows a low-magnification cross-section TEM image of a freestanding nanotube at the bottom. A stage on the substrate surface can be always found underneath each single freestanding MWNT. Its diameter is approximately the same as that of nanotube at the bottom. The outside diameter of a single freestanding MWNT at the bottom is approximately the same size of patterned nickel nanodots, which makes possible of growth of arrays of well-aligned MWNTs with smaller diameter when the patterning Ni dots are smaller. Nano-size probe energy dispersive x-ray analysis indicates that the stage is just one part of silicon

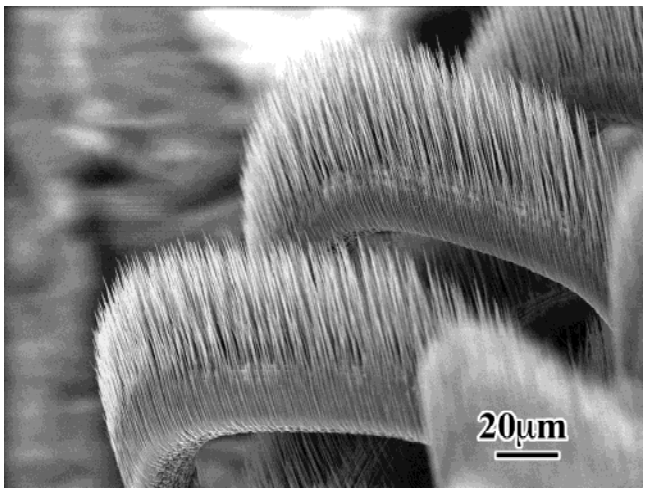

FIG. 7. SEM image of MWNTs grown on a tungsten filament coated by a thin Ni layer. Most MWNTs grow along the dc plasma direction instead of the substrate surface, even at two sides of the filament.

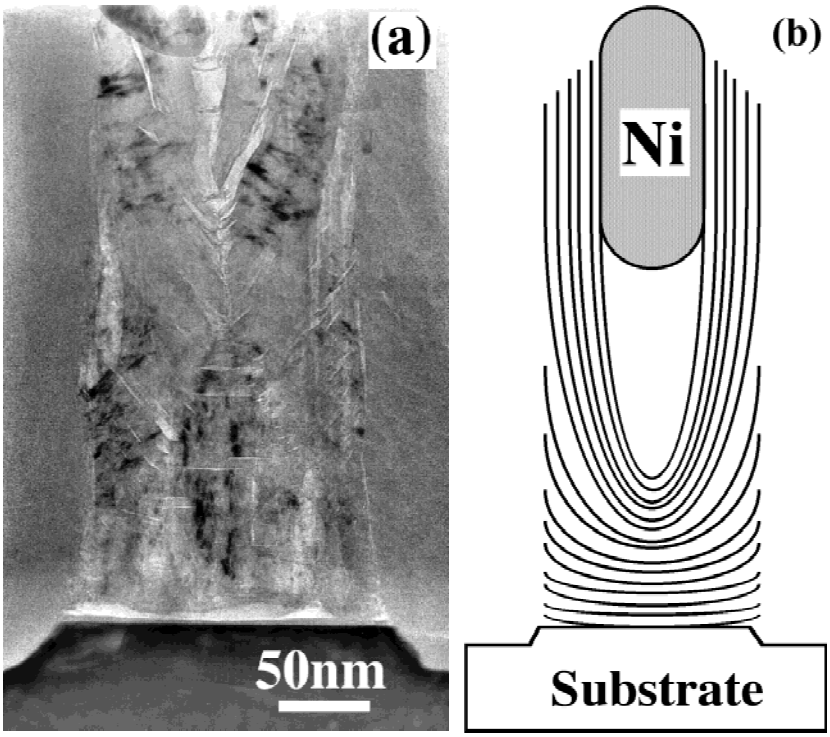

FIG. 8. (a) Cross-sectional TEM image of the bottom of a single freestanding nanotube. The size of the stage on the Si substrate is the same as the diameters of nanotubes. No Ni particles are observed at the bottom of nanotube. The change in curvature of up-opened dome structures can be seen in (a) and is schematically shown in (b).

substrate instead of a Ni particle. Since the substrate surface was smooth before the growth of nanotube, the stage was presumably formed due to plasma etching. Nickel has never been found directly on the silicon surface. The smooth substrate surface at the stage indicates no reaction between Ni and substrate Si due to low growth temperature, which is different from the result of Bower *et al.* due to high growth temperature.[22] Graphitic layers are formed underneath Ni film and lift Ni film from substrate surface. In Fig. 8(a), one can see curved white lines and bands which correspond to stacking space between graphitic up-opened domes. As schematically shown in Fig. 8(b), graphitic layers above the stage surface are flat and parallel to the substrate surface. As the spacing between dome and silicon surface increases, the flat graphitic layers gradually change into up-opened dome. The curvature of these up-opened dome structures become smaller, finally they change into hollow nanotubes above about 300 nm over the silicon substrate surface. The process that graphitic layers change from flat graphitic disks into up-opened dome structure and finally nanotube structure just reflects the Ni cylinder formation process from Ni thin film.

IV. SUMMARY

In summary, microstructures of aligned nanotubes and aligned single freestanding nanotubes were studied by electron microscopy. Microstructural studies showed that the growth of arrays of freestanding MWNTs with extremely sharp tips (2-nm radius), controlled diameter, length, and site spacing (1 and 2 μm) was achieved. It was found that the growth of MWNTs grown on a large-area Ni layer and on nickel nanodots is different, which might result from a local temperature difference at nickel nanodots and a large area Ni layer. A focusing effect of the coming bombardment ions at nickel nanodots is a possible reason for the enhancement of the local temperature. Most of the Ni particles at tips of MWNTs grown on a large area nickel layer and nickel nanodots were found to be [220] preferentially oriented. This may result from a channeling effect of ions coming into Ni particles in the dc plasma. The alignment mechanism of carbon nanotubes is suggested mainly due to electrical field at the local substrate surface, which is parallel to applied dc plasma direction in the case of large bias voltage.

ACKNOWLEDGMENTS

This material is based upon work supported in part by the United States Army Natick Soldier Systems Center under Grant No. DAAD16-00-C-9227, National Science Foundation under Grant No. DMR-9996289, and Department of Energy under Grant No. DE-FG02-00ER45805. The work performed at Yale was supported in part by Defense Advanced Research Projects Agency (DARPA).

REFERENCES

1. A.G. Rinzler, J.H. Hafner, P. Nikolaev, L. Lou, S.G. Kim, D. Tomanek, P. Nordlander, D.T. Colbert, and R.E. Smalley, Science **269,** 1550 (1995).
2. W.A. de Heer, A. Chatelain, and D.A. Ugarte, Science **270,** 1179 (1995).
3. Y. Saito, K. Hamaguchi, K. Hata, K. Uchida, Y. Tasaka, F. Ikazaki, M. Yumura, A. Kasuya, and Y. Nishina, Nature **389,** 554 (1997).
4. H. Schmid and H.W. Fink, Appl. Phys. Lett. **70,** 2679 (1997).
5. P.G. Collins and A. Zettl, Appl. Phys. Lett. **69,** 1969 (1996).
6. Z.F. Ren, Z.P. Huang, J.W. Xu, J.H. Wang, P. Bush, M.P. Siegal, and P.N. Provencio, Science **282,** 1105 (1998).
7. Z.P. Huang, J.W. Wu, Z.F. Ren, J.H. Wang, M.P. Siegal, and P.N. Provencio, Appl. Phys. Lett. **73,** 3845 (1998).
8. Z.F. Ren, Z.P. Huang, J.W. Xu, D.Z. Wang, and J.H. Wang, in *Electronic Properties of Novel Materials—Science and Technology of Molecular Nanostructures,* edited by H. Kuzmany, J. Fink, M. Mehring, and S. Roth, AIP Conference Proceedings, **486,** Tirol, Austria (Springer Verlag, The Netherlands, 1998), pp. 263–67.
9. W.Z. Li, S.S. Xie, L.X. Qian, B.H. Chang, B.S. Zou, W.Y. Zhou, R.A. Zhao, and G. Wang, Science **274,** 1701 (1996).
10. S.S. Fan, M.G. Chapline, N.R. Franklin, T.W. Tombler, A.M. Cassell, and H.J. Dai, Science **283,** 512 (1999).
11. J. Li, C. Papadopoulos, J.M. Xu, and M. Moskovits, Appl. Phys. Lett. **75,** 367 (1999).
12. J.S. Suh and J.S. Lee, Appl. Phys. Lett. **75,** 2047 (1999).
13. L. Nillson, O. Groening, C. Emmenegger, O. Kuettel, E. Schaller, L. Schlapbach, H. Kind, J-M. Bonard, and K. Kern, Appl. Phys. Lett. **76,** 2071 (2000).
14. M.H. Kuang, Z.L. Wang, X.D. Bai, J.D. Guo, and E.G. Wang, Appl. Phys. Lett. **76,** 1255 (2000).
15. C. Bower, W. Zhu, S. Jin, and O. Zhou, Appl. Phys. Lett. **77,** 830 (2000).
16. Z.F. Ren, Z.P. Huang, D.Z. Wang, J.G. Wen, J.W. Xu, J.H. Wang, L.E. Calvet, J. Chen, J.F. Klemic, and M.A. Reed, Appl. Phys. Lett. **75,** 1086 (1999).
17. J.G. Wen, in *Characterization of High-T_c Materials and Devices by Electron Microscopy,* edited by N.D. Browning and S.J. Pennycook, (Cambridge Univ. Press, Cambridge, United Kingdom, 2000), pp. 69–101.
18. Y. Saito, T. Yoshikawa, M. Inagaki, M. Tomita, and T. Hayashi, Chem. Phys. Lett. **204,** 277 (1993).
19. G. Carter and J.S. Colligon, in *Ion Bombardment of Solids,* (Heinemann Educational Books, London, United Kingdom, 1968).
20. Y. Iijima, M. Hosaka, N. Tanabe, N. Sadakata, T. Saitoh, O. Kohno, and K. Takeda, Appl. Superconductivity **4,** 475 (1996).
21. P. Poncharal, Z.L. Wang, Z. Ugarte, and W.A. de Heer, Science **283,** 1513 (1999).
22. C. Bower, O. Zhou, W. Zhu, D.J. Werder, and S. Jin, Appl. Phys. Lett. **77,** 2767 (2000).